First observation of the proton emitter 116La: Evidence for strong neutron-proton pairing from proton separation energies and emission probabilities

Wei Zhang (wezh@kth.se)
Department of Physics, Royal Institute of Technology https://orcid.org/0000-0001-8650-9956

Bo Cederwall
Department of Physics, Royal Institute of Technology

Ozge AKTAS
Department of Physics, Royal Institute of Technology https://orcid.org/0000-0003-0212-7497

Xiaoyu Liu
Department of Physics, Royal Institute of Technology

Aysegül Ertoprak
Department of Physics, Royal Institute of Technology

Ayse Nyberg
Department of Physics, Royal Institute of Technology

Kalle Auranen
Accelerator Laboratory, Department of Physics, University of Jyväskylä https://orcid.org/0000-0002-6604-7659

Betool Alayed
Department of Physics, Oliver Lodge Laboratory, University of Liverpool

Hussam Badran
Accelerator Laboratory, Department of Physics, University of Jyväskylä

Helen Boston
Department of Physics, Oliver Lodge Laboratory, University of Liverpool

Maria Doncel
Department of Physics, Stockholm University

Ulrika Forsberg
Accelerator Laboratory, Department of Physics, University of Jyväskylä

Tuomas Grahn
University of Jyväskylä https://orcid.org/0000-0002-6255-2279

Paul Greenlees
Accelerator Laboratory, Department of Physics, University of Jyväskylä

Song GUO

Institute of Modern Physics, Chinese Academy of Science https://orcid.org/0000-0003-3430-7361
Jacob Heery
Department of Physics, Oliver Lodge Laboratory, University of Liverpool
Joshua Hilton
Accelerator Laboratory, Department of Physics, University of Jyväskylä
David Jenkins
University of York
Rauno Julin
Accelerator Laboratory, Department of Physics, University of Jyväskylä
Sakari Juutinen
Accelerator Laboratory, Department of Physics, University of Jyväskylä
Minna Luoma
Accelerator Laboratory, Department of Physics, University of Jyväskylä
Olavi Neuvonen
Accelerator Laboratory, Department of Physics, University of Jyväskylä
Joonas Ojala
Accelerator Laboratory, Department of Physics, University of Jyväskylä
Robert Page
University of Liverpool
Janne Pakarinen
University of Jyväskylä https://orcid.org/0000-0001-8944-8757
Edward Paul
Department of Physics, Oliver Lodge Laboratory, University of Liverpool
Costel Petrache
CNRS/IN2P3, IJCLab, Université Paris-Saclay
Panu Rahkila
Accelerator Laboratory, Department of Physics, University of Jyväskylä
Panu Ruotsalainen
University of Jyvaskyla
Mikael Sandzelius
Accelerator Laboratory, Department of Physics, University of Jyväskylä
Jan Sarén
Accelerator Laboratory, Department of Physics, University of Jyväskylä
Stuart Szwec
Accelerator Laboratory, Department of Physics, University of Jyväskylä
Holly Tann
Department of Physics, Oliver Lodge Laboratory, University of Liverpool
Juha Uusitalo
Accelerator Laboratory, Department of Physics, University of Jyväskylä

Robert Wadsworth
University of York https://orcid.org/0000-0002-4187-3102

Article

Keywords:

Posted Date: March 8th, 2022

DOI: https://doi.org/10.21203/rs.3.rs-1358927/v1

Additional Declarations: There is **NO** Competing Interest.

Version of Record: A version of this preprint was published at Communications Physics on November 14th, 2022. See the published version at https://doi.org/10.1038/s42005-022-01069-w.

First observation of the proton emitter $^{116}_{57}La_{59}$: Evidence for neutron-proton pairing from proton separation energies and emission probabilities

W. Zhang [1, *], B. Cederwall [1, †], Ö. Aktas [1], X. Liu [1], A. Ertoprak [1], A. Ataç Nyberg [1], K. Auranen [2], B.M.A. Alayed [3,4], H. Badran [2], H. Boston [3], M. Doncel [5], U. Forsberg [2], T. Grahn [2], P. T. Greenlees [2], S. Guo [6], J. Heery [3,2], J. Hilton [2,3], D. Jenkins [7], R. Julin [2], S. Juutinen [2], M. Luoma [2], O. Neuvonen [2], J. Ojala [2], R. D. Page [3], J. Pakarinen [2], J. Partanen [2,‡], E. S. Paul [3], C. Petrache [8], P. Rahkila [2], P. Ruotsalainen [2], M. Sandzelius [2], J. Sarén [2], S. Szwec [2], H. Tann [3,2], J. Uusitalo [2], and R. Wadsworth [7]

Abstract

The discovery of the new proton emitter $^{116}_{57}La_{59}$, 23 neutrons away from the only stable La isotope, $^{139}_{57}La_{82}$, is reported. The ^{116}La nuclei were synthesised in the fusion-evaporation reaction ^{58}Ni(^{64}Zn, p4n)^{116}La and identified via their proton radioactivity using the MARA mass spectrometer and the silicon detectors placed at its focal plane. Comparisons of the measured proton energy ($E_p = 718 \pm 9$ keV) and half-life ($T_{1/2} = 50 \pm 22$ ms) with values calculated using the Universal Decay Law approach indicate that the proton is emitted with an orbital angular momentum $l = 2$ and that its emission probability is enhanced relative to its closest, less exotic, odd-even lanthanum isotope ($^{117}_{57}La_{60}$) while the proton-emission Q-value is lower. We propose this to be a signature for the presence of strong neutron-proton pair correlations in this exotic, neutron deficient system. The observations of γ decays from isomeric states in ^{116}La and ^{117}La are also reported.

Introduction. Nucleonic pair correlations, also commonly called "pairing", play an important role in the structure of atomic nuclei. Well-known manifestations of the nuclear pairing effect, which is similar to condensed-matter physics phenomena such as superconductivity and superfluidity, are the odd-even staggering of nuclear binding energies [1], seniority symmetry [2, 3, 4] in the low-lying spectra of spherical even-even nuclei, and the reduced moments of inertia and backbending effect [5, 6] in rotating deformed nuclei. The first fundamental theoretical description of pairing in condensed matter physics focused on the properties of systems composed of large numbers of fermions, such as the electrons in superconductors (Bardeen-Cooper-Schrieffer (BCS) theory [7, 8]). The same formalism can be applied to atomic nuclei if the limited number of nucleons that can be bound in such systems is properly taken into account. A basic feature of BCS theory is that it treats systems with identical fermions moving in time-reversed orbitals as correlated pairs with opposite spins ($J = 0$), so-called Cooper pairs. Mean-field models of atomic nuclei based on the BCS approach, such as Hartree-Fock-Bogoliubov theory [9], therefore treat the neutron and proton pairing fields separately. These pairing fields give rise to the nuclear odd-even mass differences for neutrons and protons independently and are called isospin $T = 1$ or isovector pairing. However, the unique coexistence of two distinct fermionic systems (neutrons and protons) in the nucleus may produce additional pairing modes not found elsewhere in Nature. In particular in nuclei with equal or nearly equal neutron and proton numbers ($N \approx Z$) enhanced correlations arise between neutrons and protons that occupy orbitals with the same quantum numbers. The normal isovector pairing mode based on like-particle neutron-neutron (nn) and proton-proton (pp) Cooper pairs can be generalized to include neutrons and protons which may then also form isospin $T = 1$, angular momentum $J = 0$ np pairs. Of special interest is the long-standing question of the possible presence of a new and structurally different np pairing mode termed isoscalar pairing [10, 11, 12, 13, 14, 15, 16, 17, 18, 19] predicted to be built from isospin $T = 0$, $J > 0$ np pair correlations. Many theoretical calculations predict that isoscalar pairing may only manifest itself clearly in the heaviest, most exotic neutron deficient nuclei with $A > 80$, for a review, see Ref. [20]. Calculations using isospin-generalized BCS and HFB equations including pp, nn, np ($T = 1$), and np ($T = 0$) Cooper pairs indicated that there may exist a second-order quantum phase transition in the ground states of $N = Z$ nuclei from $T = 1$ pairing below mass 80 to a predominantly $T = 0$ pairing phase above mass 90, with the intermediate mass 80-90 region showing a co-existence of $T = 0$ and $T = 1$

[1]Department of Physics, Royal Institute of Technology, 10691 Stockholm, Sweden
[2]Accelerator Laboratory, Department of Physics, University of Jyväskylä, FI-40014 Jyväskylä, Finland
[3]Department of Physics, Oliver Lodge Laboratory, University of Liverpool, Liverpool L69 7ZE, United Kingdom
[4]Physics Department, Qassim University, Kingdom of Saudi Arabia
[5]Department of Physics, Stockholm University, SE-10691 Stockholm, Sweden
[6]Institute of Modern Physics, Chinese Academy of Sciences, Lanzhou 730000, China
[7]Department of Physics, University of York, Heslington, York YO10 5DD, United Kingdom
[8]Université Paris-Saclay, CNRS/IN2P3, IJCLab, 91405 Orsay, France

[*]e-mail:wezh@kth.se
[†]e-mail:bc@kth.se
[‡]Deceased

pairing modes [21]. There are even predictions for a dominantly $T = 0$ ground-state pairing condensate in $N \sim Z$ nuclei around mass 130 [22].

Proton radioactivity, i.e. spontaneous and direct proton emission, is a rare nuclear decay mode observed for the ground-states or isomeric states of some extremely neutron deficient nuclides (around 30 are known to date). Ground-state proton radioactivity was first observed by Hofmann *et al.* for ^{151}Lu [23] and by Klepper *et al.* for ^{147}Tm [24]. The first observation of proton radioactivity in the region of neutron deficient nuclei above tin, was made for ^{109}I and ^{113}Cs by Gillitzer *et al.* [25]. Proton emission from odd-odd nuclides may reveal effects of the residual proton-neutron interactions between the odd valence neutron and proton [26]. It has previously been observed for a few such cases that the proton-decay Q value, Q_p, of the odd-odd nucleus is lower than that of its less-exotic neighboring odd-even isotope. This was first inferred by Page *et al.* for the ^{108,109}I pair [27] and recently confirmed by direct measurement of proton emission from ^{108}I by Auranen *et al.* [28]. Another example is the ^{112,113}Cs pair [29]. Mass models fail consistently in reproducing this behavior. This might be attributed to the attractive residual force between the odd valence neutron and proton in the odd-odd systems [27, 30] but the nature of this neutron-proton interaction is until now unknown.

Here, we present the discovery of the extremely neutron deficient, $T_Z = 1$, isotope $^{116}_{57}$La$_{59}$ via its radioactive proton decay and the observation of γ-ray transitions from low-lying microsecond isomers in ^{116,117}La. We propose that the observed differences in measured proton decay Q values and proton formation probabilities between neighboring isotopes provide a new signature and evidence for strong neutron-proton pairing in these exotic systems.

Results. The experiment was performed at the Accelerator Laboratory of the University of Jyväskylä using the ^{58}Ni(^{64}Zn, $p3n$)^{117}La and ^{58}Ni(^{64}Zn, $p4n$)^{116}La fusion-evaporation reactions. Relevant experimental details, in particular regarding the operation of the vacuum-mode recoil separator MARA (Mass Analysing Recoil Apparatus) and the energy calibration of the double-sided silicon strip detector (DSSD) placed at the MARA focla plane, are described in Methods.

Fig. 1 shows the decay energy spectra recorded in the DSSD at the beam energy of 330 MeV. The corresponding events were punch-through vetoed and with the requirement that the decay occurred within 100 ms after the implantation of a recoil in the same DSSD quasipixel as well as with the requirement that the multiplicity of evaporated charged particles detected in JYTube (Jyväskylä-York Tube) was 0 or 1. The high background in the low-energy region is mainly from β decays of strongly populated nuclides closer to the stability line. The peak at 808(5) keV corresponds to the proton decay of ^{117}La and its half-life was measured to be $T_{1/2} = 21.6(31)$ ms, in agreement with the previous measurements of the ground-state proton decay of ^{117}La [31, 32, 33]. The yield of ~ 680 counts in this peak corresponds

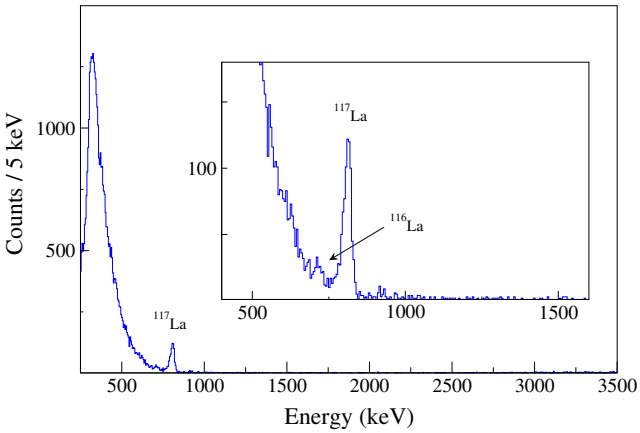

Figure 1: Energy spectrum registered in the DSSD at the beam energy 330 MeV for punch-through-vetoed decay events occurring within 100 ms after an ion implantation. The inset shows the enlarged low-energy region. The previously known proton-decay peak of ^{117}La and the newly discovered proton-decay peak of ^{116}La are indicated. See the main text and Methods for details.

to a production cross section of ~ 120 nb, assuming a MARA transmission efficiency of 35% for mass 117.

The low-energy region of the spectrum in Fig. 1 is enlarged and shown in the inset. A small peak at 718(9) keV is clearly visible above the β background with a statistics of 40(14) counts, which we assign to the ground-state proton decay of ^{116}La. These proton-decay events could be further enhanced relative to the β-decay background by requiring that they occurred in delayed coincidence with γ rays at the focal plane of MARA, as explained in Methods. A half-life of $T_{1/2} = 50(22)$ ms was determined for the proton decay of ^{116}La (Methods).

Recoil-γ-decay event chains were investigated in order to search for isomeric γ-ray transitions in ^{117}La and the newly discovered isotope ^{116}La. The γ-ray energy spectrum recorded by the clover high-purity germanium (HPGe) detectors sourrounding the MARA focal plane for events registered within 8 μs of a recoil implantation and gated by ^{117}La protons (Figure 2(a)), reveals a peak with 9 counts at 192 keV. Based on a maximum likelihood analysis [34], a lifetime $\tau = 3.9^{+1.9}_{-0.9}$ μs ($T_{1/2} = 2.7^{+1.3}_{-0.7}$ μs) was determined for the corresponding isomeric level. Using Weisskopf estimates, we assign the multipolarity of the 192 keV transition to be of magnetic quadrupole (M2) character (see Methods for details). A tentative spin-parity $7/2^-$ is consequently assigned to the 192 keV level, based on the previous assignment of the ground state as $(3/2^+)$ [31, 33]. The intensity of the observed 192 keV transition indicates an isomeric population ratio of the order of 30%. This would be in agreement with the observation of prompt γ rays from ^{117}La by Liu *et al.* [33] if a significant fraction of those γ rays emanate from a rotational cascade feeding the isomer. Evidence for an isomeric M2 transition at an energy of 182 keV was also observed to be correlated with the proton decay of ^{116}La, as shown in Figure 2(b). Its half-life was determined to be

$T_{1/2} = 2.0^{+2.8}_{-0.8}$ μs.

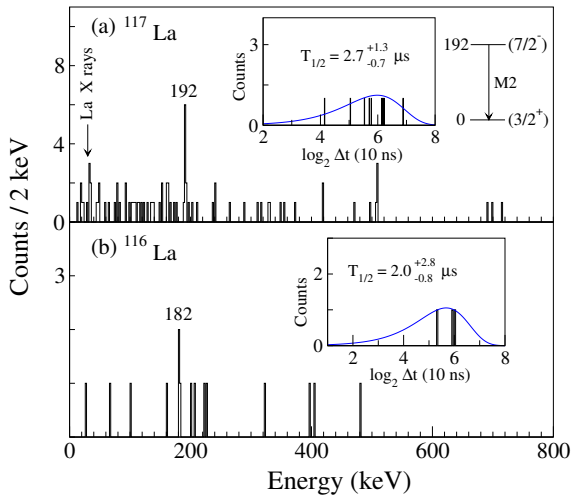

Figure 2: (a) γ-ray energies detected within 8 μs of a recoil implantation into the DSSD and followed by a proton decay from ^{117}La in the same quasipixel. The inset shows the time distribution of 192-keV γ-rays selected in this way. The fit of the lifetime using the maximum likelihood method [34] is indicated by the blue curve. The proposed corresponding level scheme obtained for ^{117}La is indicated to the right. (b) Same as (a) tagged by ^{116}La proton decays and for 182-keV γ-rays.

Discussion. The ground-state and low-lying yrast configurations of the neutron deficient lanthanum isotopes are predicted to be moderately quadrupole-deformed ($\beta_2 \approx 0.3$) [35] and based on valence protons occupying Nilsson [36] orbits from the near-degenerate $2d_{5/2}$ and $1g_{7/2}$ sub-shells. Levels based on configurations with $g_{9/2}/h_{11/2}$ spherical parentage that extrude/intrude with increasing deformation may also come close to the Fermi level. The detailed balance determining which configuration actually forms the ground state may provide important input for stringent tests of effective nucleon-nucleon interactions used in current nuclear models. This situation also provides the necessary requirements for nuclear isomerism created by yrast spin traps [38, 37]. The relevant Nilsson configurations near the Fermi level have been discussed extensively in the literature for neighboring isotopes closer to the line of beta stability, see e.g. the recent work on ^{119}Cs [39]. In ^{121}La, the most neutron deficient lanthanum isotope for which excited states have been identified to date, two rotational bands have been observed and assigned to be built on the $9/2^+[404]$ and $1/2^-[550]$ Nilsson orbitals [40].

In theoretical studies of the proton emission rate from ^{117}La the adiabatic approach [41] suggested ground-state spin-parity $J^\pi = 3/2^+$ [31], while non-adiabatic calculations [42, 43] proposed $J^\pi = 3/2^+$ or $J^\pi = 3/2^-$. The $J^\pi = 3/2^+$ assignment corresponds to the $3/2^+[422]$ Nilsson orbital [39] of mainly $2d_{5/2}$ parentage and hence emission of predominantly $l = 2\hbar$ protons. On the other hand, $J^\pi = 3/2^-$ would correspond to the $3/2^-[541]$ $1h_{11/2}$ intruder configuration [39] and, consequently, $l = 5\hbar$ proton emission which would be expected to be subject to additional strong hindrance due to the larger centrifugal barrier. For the proton emitter ^{121}Pr, it was proposed [44] that the $J^\pi = 7/2^-$ member of such a configuration could form the ground state as a result of a strong Coriolis interaction, i.e. a kinematic coupling of the angular momenta of the odd valence proton and the core. Even if this state is unlikely to form the ground state of ^{117}La it may well produce a low-lying excited state resulting in a spin-trap isomer. The 192-keV M2 transition found in this work is therefore assigned to populate the $3/2^+$ ground state from this $7/2^-$ state as indicated in Figure 2. For ^{116}La, the spin-parity of its ground-state is considerably more difficult to assess due to the numerous possibilities to couple the low-lying proton and neutron configurations. Therefore, even though the 182-keV M2 isomeric transition is most likely of similar character, it was therefore not placed into a tentative level scheme.

The Universal Decay Law is a convenient, model independent microscopic approach to quantum tunneling theory which can be applied to all forms of ground-state to ground-state radioactive decays involving the emission of protons and heavier charged particles [45, 46]. Within this formalism the half-life can be expressed as

$$T_{1/2} = \frac{\hbar \ln 2}{\Gamma_l} = \frac{\ln 2}{\upsilon} \left| \frac{H_l^+(\chi,\rho)}{RF_l(R)} \right|^2 \qquad (1)$$

where l is the angular momentum carried by the emitted particle and υ is its outgoing velocity. In the case of proton emissiion, the distance parameter, R, denotes the point where the radial wave function describing the proton in the internal region of the nucleus is matched with its outgoing wave function. H_l^+ is the Coulomb-Hankel function which can be well approximated by the Wentzel-Kramers-Brillouin (WKB) value [47]. The formation probability, $|RF_l(R)|^2$, that can be extracted from Eq. 1 can provide a more precise evaluation of the influence of the nuclear structure on the proton decay width, especially in the case of a deformed nucleus [46].

Figure 3 shows the $|RF_l(R)|^2$ values as extracted from the experimental half-lives and Q values from the ground-state proton-decays observed to date in odd-Z elements between $Z = 53$ and 83 [28, 49, 48]. In the present analysis it was not possible to accurately measure the β-decay branching ratio for the ground-state decay of ^{116}La. Based on the theoretical calculations by Möller *et al.*, which predicted a partial β-decay half-life of 124 ms for ^{116}La [50], the proton-decay branching ratio is estimated to be 60(18)% and, consequently, the partial proton-decay half-life is deduced as $T_{1/2,p} = 84^{+86}_{-50}$ ms. The formation probability for ^{116}La is furthermore calculated under two alternative assumptions, that the orbital angular momentum carried by the emitted proton is $l_p = 2\hbar$ or $l_p = 4\hbar$, while $l_p = 0$, $l_p = 1\hbar$ and $l_p = 3\hbar$ have been excluded based on the lack of proton orbitals with s, p or f parentage close to the Fermi level. It is clearly seen from Figure 3 that a reasonable value for

the formation probability in the proton decay of ^{116}La can only be obtained when $l = 2\hbar$. This firmly assigns the proton component of the ground-state wave function of ^{116}La to be of predominantly $d_{5/2}$ parentage, which is consistent with the results for ^{117}La derived in the present work as well as the neighboring proton-emitters $^{108,109}_{53}$I, $^{112,113}_{55}$Cs, $^{121}_{59}$Pr, and $^{130,131}_{63}$Eu [48].

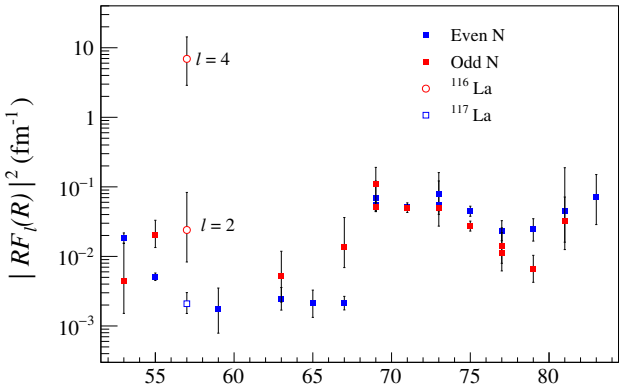

Figure 3: Deduced proton formation probabilities, $|RF_l(R)|^2$, for the ground-state decays in the odd-Z elements between $Z = 53$ and 83 as a function of the proton number Z. The Q_p values and half-lives for ^{116,117}La are from the results obtained in the present work. The remaining experimental data used for this plot are taken from Ref. [48] as well as from the recently reported results on ^{108}I [28] and ^{185}Bi [49]. Experimental uncertainties in the half-lives and Q-values have been taken into account when calculating the error bars of the formation probabilities. The formation probability for ^{117}La has been calculated using the proton orbital angular momentum $l_p = 2\hbar$ and for ^{116}La using two alternative values, $l_p = 2\hbar$ and $l_p = 4\hbar$. For ^{116}La, the partial proton-decay half-life was calculated based on the theoretically predicted β-decay partial half-life of 124 ms [50]. Information on the values of l_p, Q_p and half-lives used for the calculation as well as the derived formation probabilities for other proton-emitters can be found in Table II of Ref. [51].

It can be observed that the proton formation probabilities shown in Figure 3, are divided into two main regions at $Z = 69$, where $|RF_l(R)|^2$ reaches the maximum value for the nucleus $^{144}_{69}$Tm. Focusing first on the even-N nuclides in the region with $Z \geq 69$ they have consistently the largest $|RF_l(R)|^2$ values with a dip appearing around $_{77}$Ir - $_{79}$Au. The behavior is associated with the nuclear deformation of these proton emitters which are predicted to be spherical or weakly-deformed in this region [35] and the ground-state proton wave function to be dominated by a single-particle orbit [51, 52]. Consequently, the formation probability of this region is generally large, and the dip in $|RF_l(R)|^2$ around the iridium and gold proton emitters is likely related to the transitional onset of weakly-deformed shapes [35]. For the proton emitters with $Z < 69$ the $|RF_l(R)|^2$ values are consistently around one order of magnitude smaller and it was noted that this may be expected in this deformed region [47] for which the decay primarily involves only the low- l components of the deformed ground-state configuration [53, 41, 52]. However, the deformation effect on the formation probability seems to saturate already at moderate deformations since the $|RF_l(R)|^2$ values exhibit a nearly constant trend also beyond the strongly deformed $_{63}$Eu - $_{67}$Ho rare-earth nuclei. For the weakly deformed $_{53}$I - $_{55}$Cs nuclei the $|RF_l(R)|^2$ values again start increasing as a function of decreasing Z, approaching the spherical shapes close to the doubly-magic, self-conjugate nucleus $^{100}_{50}$Sn$_{50}$.

Turning now to the odd-odd isotopes, a striking effect is visible in Figure 3, namely that three of the odd-N isotopes in the deformed region; $^{112}_{55}$Cs, $^{116}_{57}$La, and $^{140}_{67}$Ho have significantly larger $|RF_l(R)|^2$ values than the closest, less exotic, even-N isotope. This implies that the presence of the odd valence neutron induces a facilitating effect on the proton emission in these odd-odd systems compared with the neighboring isotope where all neutrons are paired. At the same time, the differences between the ground-state to ground-state proton-decay Q values of the odd-N proton-emitters and their less exotic nearest even-N isotopes, $\Delta Q_p^{oe} = Q_p^N - Q_p^{N+1}$($N$ odd), are negative: $\Delta Q_p^{oe} = -153(8)$ keV for $^{112,113}_{55}$Cs, -90(10) keV for $^{116,117}_{57}$La, and -83(11) keV for $^{140,141}_{67}$Ho. We also note that while $\Delta Q_p^{oe} = -222(14)$ keV for $^{108,109}_{53}$I the difference between the corresponding $|RF_l(R)|^2$ values is within the experimental uncertainties and therefore inconclusive.

The enhanced $|RF_l(R)|^2$ values for these odd-odd proton emitters and the corresonding negative ΔQ_p^{oe} values for $^{112,113}_{55}$Cs, $^{116,117}_{57}$La, and $^{140,141}_{67}$Ho isotopic pairs stand out by themselves. The *coincidence* of these quantities is even more remarkable and seems to require an explanation beyond the current understanding of proton radioactivity.

We have considered various mechanisms that might explain the observed effect and find that a possible scenario involves neutron-proton pairing effects, which may be enhanced in extremely neutron deficient nuclei for which neutron and proton numbers are approximately equal and neutrons and protons near the Fermi level therefore move in similar orbits. The properties of odd-odd nuclides are of particular interest in this sense since like-particle pair correlations are expected to be blocked by the odd valence particles.

How could then an enhanced *np* pairing strength contribute to these effects? As discussed above, a sufficient number of valence neutrons and protons moving in identical orbits may produce an *np* pairing condensate that could increase the binding of exotic, extremely neutron deficient odd-odd systems compared with those situated further down in the valley of β stability. But such an effect could also be a result of a strong attractive residual *np* interaction as discussed in earlier work [29]. The enhancement of the $|RF_l(R)|^2$ values for the odd-odd proton emitters, which indicate that the odd neutron facilitates the emission of the proton instead of binding it stronger, seems, however, at first glance contradictory to a situation with an increased binding

of the same due to a strong residual *np* interaction between the two valence nucleons. On the other hand, for a large *np* pair gap of the isovector type one may expect properties similar to "normal" isovector pairing of the like-particle type. Such pair correlations have commonly been assumed to become especially important at the nuclear surface, but there are few rigorous treatments of this difficult problem. In a study of the spatial distribution of isovector pairing strength within the HFB approach, Sandulescu *et al.* [54] calculated the neutron pairing density for the chain of even-even tin isotopes between doubly-magic $^{100}_{50}\mathrm{Sn}_{50}$ to $^{132}_{50}\mathrm{Sn}_{82}$. While the probability density for d-wave particles, which are relevant for the considered proton emitters, was predicted to be at a minimum at the nuclear surface, the pairing density was found to be sustained throughout the nucleus and with a clear enhancement at the surface. In a subsequent study, Vigezzi *et al.* [55] investigated the spatial distribution of the pairing density in ^{120}Sn using a bare nucleon-nucleon potential approach as well as with a pairing interaction induced by the exchange of collective vibrations. The resulting pairing density was found to be strongly peaked on the nuclear surface.

We propose that a mechanism by which proton emission in an odd-odd nucleus could be enhanced is via an isovector *np* pairing condensate and its modifying effects on the valence proton wave function. This might result in a more surface-peaked proton density distribution, thereby facilitating the tunneling process through the Coulomb and centrifugal barriers. A dynamic enhancement of the proton emission probability involving *np* pairs scattering into proton continuum states could also play a role in such a process. The fact that the effect is not observed in the region of near-spherical or weakly deformed nuclei is consistent with a smaller pairing gap in these nuclei while the deformed region with its higher level density and larger pairing gap, as well as closer proximity to the $N = Z$ line seems more favorable. The absence of a sizeable effect for the $^{130,131}_{63}$Eu pair is then readily explained as a result of the neutron and proton Fermi levels being situated in single-particle orbitals emanating from different major oscillator shells [56], thereby reducing neutron-proton correlations.

Whether the observed effect could also be explained by *np* pairing of the *isoscalar* type is a possibility that requires theoretical model development beyond the current state of the art. These observations highlight the importance of proton emission as a probe of fundamental nuclear structure and illustrate the need for pushing the experimental boundaries of proton emission measurements further.

Conclusions. The extremely neutron deficient isotope ^{116}La has been discovered via its ground-state proton emission (E_p = 718(9) keV, $T_{1/2}$ =50(22) ms). The proton decay of ^{117}La has also been remeasured (E_p = 808(5) keV, $T_{1/2}$ = 21.6(31) ms). Isomeric transitions of M2 character belonging to ^{117}La and ^{116}La were observed with energies and corresponding half-lives (E_γ = 192 keV, $T_{1/2} = 2.7^{+1.3}_{-0.7}$ μs) and (E_γ = 182 keV, $T_{1/2} = 2.0^{+2.8}_{-0.8}$ μs), respectively. An enhanced proton emission probability for ^{116}La as well as for a few other odd-odd proton emitters compared with their neighboring, less-exotic, odd-even isotopes is observed and found to coincide with negative ΔQ_p^{oe} values in the same cases. This unexpected effect is proposed as a manifestation of strong neutron-proton pairing of the isovector type in these systems.

References

[1] Heisenberg, W. Über den bau der atomkerne. *Z. Phys.* **78**, 156-164 (1932).

[2] De Shalit, A. & Talmi, I. *Nuclear Shell Theory* (Academic Press, New York, 1963).

[3] Talmi, I. *Simple Models of Complex Nuclei.* (Harwood Academic Press, Switzerland, 1993).

[4] Rowe, D. & Rosensteel, G. Partially Solvable Pair-coupling models with seniority-conserving interactions. *Phys. Rev. Lett.* **87**, 172501 (2001).

[5] Johnson, A., Ryde, H. & Sztarkier, J. Evidence for a "singularity" in the nuclear rotational band structure. *Phys. Lett. B* **34**, 605-608 (1971).

[6] Stephens, F. & Simon, R. Coriolis effects in the yrast states. *Nucl. Phys. A* **183**, 257-284 (1972).

[7] Bardeen, J., Cooper, L. N. & Schrieffer, J. R. Microscopic theory of superconductivity. *Phys. Rev.* **106**, 162 (1957).

[8] Bardeen, J., Cooper, L. N. & Schrieffer, J. R. Theory of superconductivity. *Phys. Rev.* **108**, 1175 (1957).

[9] Dobaczewski, J., Flocard, H. & Treiner, J. Hartree-Fock-Bogoliubov description of nuclei near the neutron-drip line. *Nucl. Phys. A* **422**, 103-139 (1984).

[10] Engel, J., Langanke, K. & Vogel, P. Pairing and isospin symmetry in proton-rich nuclei. *Phys. Lett. B* **389**, 211-216 (1996).

[11] Engel, J., Pittel, S., Stoitsov, M., Vogel, P. & Dukelsky, J. Neutron-proton correlations in an exactly solvable model. *Phys. Rev. C* **55**, 1781 (1997).

[12] Civitarese, O., Reboiro, M. & Vogel, P. Neutron-proton pairing in the BCS approach. *Phys. Rev. C* **56**, 1840 (1997).

[13] Goodman, A. L. Hartree-Fock-Bogoliubov theory with applications to nuclei. *Adv. Nucl. Phys.* **11**, 263 (1979).

[14] Satuła, W. & Wyss, R. Microscopic structure of fundamental excitations in N=Z nuclei. *Phys. Rev. Lett.* **87**, 052504 (2001).

[15] Martínez-Pinedo, G., Langanke, K. & Vogel, P. Competition of isoscalar and isovector proton-neutron pairing in nuclei. *Nucl. Phys. A* **651**, 379-393 (1999).

[16] Warner, D. D., Bentley, M. A. & Van Isacker, P. The role of isospin symmetry in collective nuclear structure. *Nat. Phys.* **2**, 311-318 (2006).

[17] Cederwall, B. et al. Evidence for a spin-aligned neutron-proton paired phase from the level structure of ^{92}Pd. *Nature* **469**, 68-71 (2011).

[18] Cederwall, B. et al. Isospin properties of nuclear pair correlations from the level structure of the self-conjugate nucleus ^{88}Ru. *Phys. Rev. Lett.* **124**, 062501 (2020).

[19] Liu, X. et al. Evidence for enhanced neutron-proton correlations from the level structure of the N=Z+1 nucleus $^{87}_{43}\mathrm{Tc}_{44}$. *Phys. Rev. C* **104**, L021302 (2021).

[20] Frauendorf, S. & Macchiavelli, A. O. Overview of neutron-proton pairing. *Prog. Part. Nucl. Phys.* **78**, 24-90 (2014).

[21] Goodman, A. L. Proton-neutron pairing in Z = N nuclei with A = 76–96. *Phys. Rev. C* **60**, 014311 (1999).

[22] Gezerlis, A., Bertsch, G. F. & Luo, Y.L. Mixed-Spin Pairing condensates in heavy nuclei. *Phys. Rev. Lett.* **106**, 252502 (2011).

[23] Hofmann, S. et al. Proton radioactivity of ^{151}Lu. *Z. Phys. A* **305**, 111-123 (1982).

[24] Klepper, O. et al. Direct and beta-delayed proton decay of very neutron-deficient rare-earth isotopes produced in the reaction ^{58}Ni + ^{92}Mo. *Z. Phys. A* **305**, 125-130 (1982).

[25] Gillitzer, A., Faestermann, T., Hartel, K., Kienle, P. & Nolte, E. Groundstate proton radioactivity of nuclei in the tin region. *Z. Phys. A* **326**, 107-119 (1987).

[26] Woods, P. J. & Davids, C. N. Nuclei beyond the proton drip-line. *Annu. Rev. Nucl. Part. Sci.* **47**, 541-590 (1997).

[27] Page, R. D. et al. Evidence for the alpha decay of ^{108}I. *Z. Phys. A* **338**, 295-301 (1991).

[28] Auranen, K. et al. Proton decay of ^{108}I and its significance for the termination of the astrophysical *rp*-process. *Phys. Lett. B* **792**, 187-192 (2019).

[29] Page, R. D. et al. Decays of odd-odd N-Z=2 nuclei above ^{100}Sn: The observation of proton radioactivity from ^{112}Cs. *Phys. Rev. Lett.* **72**, 1798 (1994).

[30] Patial, M., Arumugam, P., Jain, A. K., Maglione, E. & Ferreira, L. S. Nonadiabatic quasiparticle approach for deformed odd-odd nuclei and the proton emitter ^{130}Eu. *Phys. Rev. C* **88**, 054302 (2013).

[31] Soramel, F. et al. New strongly deformed proton emitter: ^{117}La. *Phys. Rev. C* **63**, 031304(R) (2001).

[32] Mahmud, H. et al. Proton radioactivity of ^{117}La. *Phys. Rev. C* **64**, 031303(R) (2001).

[33] Liu, Z. et al. Structure of the proton emitter ^{117}La studied by proton and γ-ray spectroscopy. *Phys. Lett. B* **702**, 24-27 (2011).

[34] Schmidt, K. H. et al. Some remarks on the error analysis in the case of poor statistics. *Z. Phys. A* **316**, 19-26 (1984).

[35] Möller, P., Sierk, A. J., Ichikawa, T. & Sagawa, H. Nuclear ground-state masses and deformations: FRDM(2012). *At. Data Nucl. Data Tables* **109-110**, 1-204 (2016).

[36] Nilsson, S. G. Binding states of individual nucleons in strongly deformed nuclei. *Dan. Mat. Fys. Medd.* **29**, 16 (1955).

[37] Jain, A. K. et al. Atlas of nuclear isomers. *Nucl. Data Sheets* **128**, 1-130 (2015).

[38] Liu, H. L., Xu, F. R., Xu, S. W., Wyss, R. & Walker, P. M. High-spin isomeric structures in exotic odd-odd nuclei: Exploration of the proton drip line and beyond. *Phys. Rev. C* **76**, 034313 (2007).

[39] Zheng, K. K. et al. Complete set of proton excitations in ^{119}Cs. *Phys. Rev. C* **104**, 044305 (2021)

[40] Cederwall, B. et al. Neutron and proton $h_{11/2}$ alignment effects in ^{121}La. *Z. Phys. A* **338**, 463-464 (1991).

[41] Maglione, E., Ferreira, L. S. & Liotta, R. Proton emission from deformed nuclei. *Phys. Rev. C* **59**, R589 (1999).

[42] Barmore, B., Kruppa, A. T., Nazarewicz, W. & Vertse, T. Theoretical description of deformed proton emitters: Nonadiabatic coupled-channel method. *Phys. Rev. C* **62**, 054315 (2000).

[43] Esbensen, H. & Davids, C. N. Coupled-channels treatment of deformed proton emitters. *Phys. Rev. C* **63**, 014315 (2001).

[44] Lopes, M. C., Maglione, E. & Ferreira, L. S. Evidence for partial rotation alignment in proton emitting ^{121}Pr. *Phys. Lett. B* **673**, 15-18 (2009).

[45] Qi, C., Xu, F. R., Liotta, R. J. & Wyss, R. Universal decay law in charged-particle emission and exotic cluster radioactivity. *Phys. Rev. Lett.* **103**, 072501 (2009).

[46] Delion, D. S. *Theory of Particle and Cluster Emission* (Springer-Verlag, Berlin, 2010).

[47] Delion, D. S., Liotta, R. J. & Wyss, R. Systematics of proton emission. *Phys. Rev. Lett.* **96**, 072501 (2006).

[48] Blank, B. & Borge, M. J. G. Nuclear structure at the proton drip line: Advances with nuclear decay studies. *Prog. Part. Nucl. Phys.* **60**, 403-483 (2008).

[49] Doherty, D.T. et al. Solving the puzzles of the decay of the heaviest known proton-emitting nucleus ^{185}Bi. *Phys. Rev. Lett.* **127**, 202501 (2021).

[50] Möller, P., Mumpower, M. R., Kawano, T. & Myers, W. D. Nuclear properties for astrophysical and radioactive-ion-beam applications (II). *At. Data Nucl. Data Tables* **125**, 1-192 (2019).

[51] Qi, C., Delion, D. S., Liotta, R. J. & Wyss, R. Effects of formation properties in one-proton radioactivity. *Phys. Rev. C* **85**, 011303(R) (2012).

[52] Qi, C., Liotta, R. & Wyss, R. Recent developments in radioactive charged-particle emissions and related phenomena. *Prog. Part. Nucl. Phys.* **105**, 214-251 (2019).

[53] Maglione, E., Ferreira, L. S. & Liotta, R. Nucleon decay from deformed nuclei. *Phys. Rev. Lett.* **81**, 538 (1998).

[54] Sandulescu, N., Schuck, P. & Viñas, X. Nuclear pairing: Surface or bulk? *Phys. Rev. C* **71**, 054303 (2005).

[55] Vigezzi, E. et al. Spatial dependence of the pairing gap in superfluid nuclei. *AIP Conference Proceedings* **1120**, 92 (2009).

[56] Ferreira, L. S., Maglione, E., & Ring, P. Covariant density functional theory for decay of deformed proton emitters: A self-consistent approach. *Phys. Lett. B* **753**, 237 (2016).

Methods

Experimental details. The ^{64}Zn beam was accelerated by the K130 cyclotron and used to impinge upon an isotopically enriched (99.8%) metallic target foil of ^{58}Ni with an areal density of 750 μg cm^{-2}. During the main production run (39 h of irradiation time) the beam kinetic energy was 330 MeV with an average intensity of 4.8 pnA. The charged-particle detector array JYTube [57] was arranged at the target position to detect evaporated charged particles emitted in the reactions. The fusion residues recoiled out of the target, and were transmitted and separated according to their mass to electric charge state ratio, A/q, to the focal plane detector system of the vacuum-mode recoil separator MARA [58]. The electric and magnetic dipole fields of MARA were set to accept fusion residues with mass $A = 117$ and (nominally) charge state $q = 30.5^+$ for the central "reference" trajectory and to accept recoils in four charge states from 29^+ to 32^+. At the MARA focal plane, recoils were passed through a position-sensitive multiwire proportional counter before being implanted into a DSSD [57, 58]. The DSSD was 300 μm thick, with an active area of 128 mm × 48 mm, and was electrically segmented into 72 vertical strips in the y plane and 192 horizontal strips in the x plane, giving a total of 13824 quasipixels. A second layer of silicon with a thickness of 500 μm was located directly behind the DSSD to veto punch-through events due to uncorrelated high-energy light charged particles and to detect β particles escaping after leaving a partial energy signal in the DSSD. Five clover HPGe detectors were placed surrounding the focal plane of MARA in a close-packed geometry and used for the measurement of delayed γ rays following recoil implantations and/or charged particle decays detected in the DSSD. All detector signals were time stamped using a global 100 MHz clock and recorded independently by the triggerless data acquisition system [59]. The data were analyzed online and offline using the GRAIN software package [60].

The energy calibration of the DSSD was accomplished using a standard mixed-isotope (^{241}Am, ^{244}Cm, ^{239}Pu) α radioactive source with its three main α-energy peaks, as well as in-beam data for the known proton decay of ^{109}I [48], its α-decaying daughter ^{108}Te, and the α-emitters ^{109}Te and ^{110}I [61]. The ^{109,110}I and ^{108,109}Te ions were produced in reactions using a higher beam energy of 370 MeV in a brief run after the main experiment, see the corresponding characteristic proton and alpha decay peaks in Fig. 4.

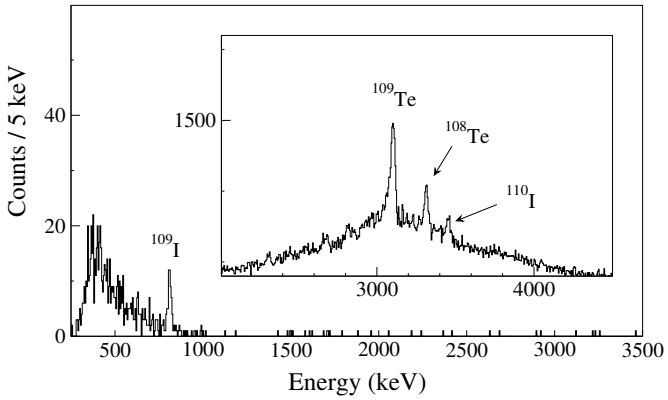

Figure 4: Energy spectrum registered in the DSSD at the beam energy of 370 MeV for punch-through-vetoed decay events ocurring within 300 μs of an ion implantation into the same DSSD quasipixel. The proton-decay peak of ^{109}I is indicated. The inset shows α-decay peaks from ground-state decays of ^{110}I and ^{108,109}Te obtained by applying a recoil-decay correlation time of 3 s.

Weisskopf estimates. The single-particle estimates provide a reasonable relative comparison of electromagnetic transition rates and allow ones to make some gerneral predictions about which multipole is most likely to be emitted [62]. The estimates for mean half-lives used in this work are as follows

$$\tau(\mathrm{M2}) = \frac{1}{3.5 \times 10^7 A^{2/3} E_\gamma{}^5} \ \mathrm{s}$$
$$\tau(\mathrm{E3}) = \frac{1}{3.39 \times 10^1 A^2 E_\gamma{}^7} \ \mathrm{s} \qquad (2)$$
$$\tau(\mathrm{E2}) = \frac{1}{7.28 \times 10^7 A^{4/3} E_\gamma{}^5} \ \mathrm{s}$$

where A is the mass number and E_γ is the energy of the γ-ray in MeV. For the new observed 192-keV isomeric-γ ray for ^{117}La, the estimated lifetime of an M2 transition is 4.6 μs

which is in fair agreement with the measured lifetime $3.9^{+1.9}_{-0.9}$ μs. In contrast, the lifetime for a state depopulated entirely by an E3 transition of the same energy would be 0.22 s, while the estimated lifetime of an E2 transition would be 0.09 μs (equivalent to about one fifth of the flight time through the MARA separator). The isomeric state is most likely situated at 192 keV excitation energy since there are no significant other peaks present in the spectrum of Fig. 2(a), apart from La X-rays which are expected due to internal conversion of the M2 transition.

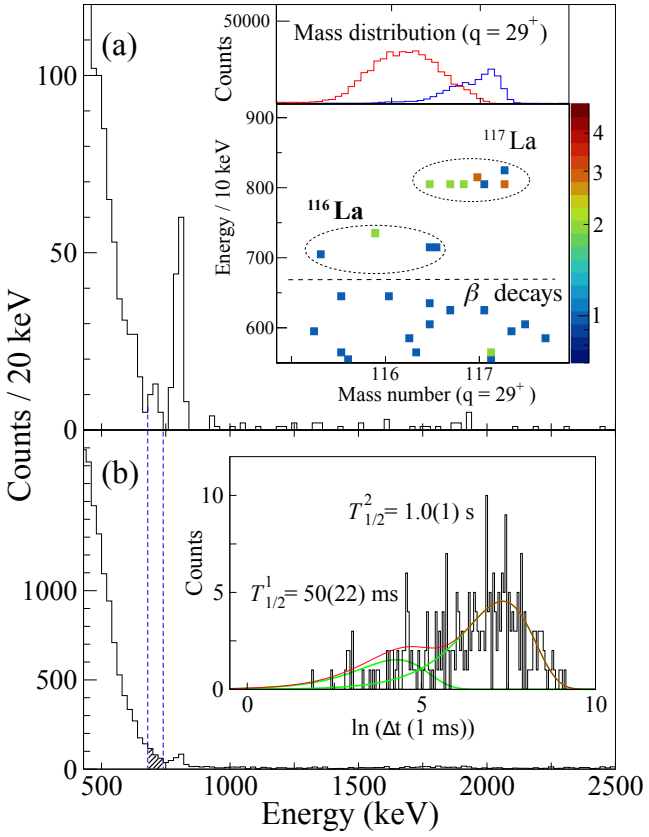

Figure 5: Projected decay energy spectrum measured in the DSSD for events correlated with a prior detection of a recoil-γ event. (a) The decay events were required to occur within 100 ms after recoil implantation into the same DSSD quasipixel. The lower inset shows the two-dimensional distribution of ion mass vs decay energy for ions in charge state $q = 29^+$. The upper inset shows the mass distributions of ^{116}I and ^{117}Xe ions from the same experiment measured in MARA drawn in red and blue, respectively. (b) The decay events were measured within 10 s of a recoil implantation. The blue dashed lines are drawn to illustrate the location of the proton peak of ^{116}La, as indicated by the shaded area. The inset shows the logarithmic time spectrum of the decay events in the shaded region, fitted using a two-component function (red). The green curves show each fitted component. The distribution of higher ln($\triangle$t) values corresponds to the random-correlated β-ray background with its effective fitted half-life.

Mass and half-life determinations for the proton decay of ^{116}La. Figure 5 (a) displays the energy spectrum for decay events occurring within 100 ms of a recoil implantation in the DSSD and in delayed coincidence with recoil-decay-correlated isomeric γ rays. In this way, the dominant β background in the DSSD spectra could be greatly reduced and the new proton peak assigned to ^{116}La becomes more pronounced. The inset shows a two-dimensional spectrum of decay energy versus ion mass number, where only ions with charge state 29^+ were selected. For this charge state the recoil implantation rate was substantially lower with a correspondingly lower burden of random correlations between the implantation of fusion residues and β rays. The upper part of the inset to Fig. 5 (a) shows the measured mass distributions for recoils with mass 116 and 117 in the same charge state. The distributions drawn in red and blue correspond to the strongly populated nuclides ^{116}I and ^{117}Xe, respectively, which are obtained by gating on their characteristic isomeric γ rays. In the two-dimensional histogram of energy vs mass the high-energy group corresponds to the ground-state proton decays of ^{117}La, while the low-energy distribution corresponds to β-decay events. The five events in the middle group coincide with the distribution for ions with mass 116 and with the proton line of the new isotope ^{116}La. Panel (b) shows decays within 10 s of a recoil implantation. Using the logarithmic binning method described by Schmidt *et al.* [34, 63], a two-component function was used to fit the lifetime of the decay events within the shaded region of Fig. 5 (b). This function is given by

$$|\frac{dn}{d\theta}| = (n_1\lambda_1 e^{-\lambda_1 e^{\theta}} + n_2\lambda_2 e^{-\lambda_2 e^{\theta}})e^{\theta}. \quad (3)$$

where $\theta = ln(\triangle t)$ and $\triangle$t is the correlation time between decay and recoil and in the unit of ms, n_i and λ_i are the number of counts and decay constants corresponding to the true and random-correlated distributions as shown in the inset of Fig. 5 (b).

Data availability. Raw data were obtained at the Accelerator Laboratory, University of Jyväskylä, Finland. All other derived data used to support the findings of this study are available from the corresponding authors upon request.

References

[57] Uusitalo, J., Sarén, J., Partanen, J. & Hilton, J. Mass analyzing recoil apparatus, MARA. *Acta Physica Polonica B* **50**, 319-327 (2019).

[58] Sarén, J. et al. The new vacuum-mode recoil separator MARA at JYFL. *Nucl. Instr. Meth. Phys. Res. A* **266**, 4196-4200 (2008).

[59] Lazarus, I. et al. The GREAT triggerless total data readout method. *IEEE Trans. Nucl. Sci.* **48**, 567-569 (2001).

[60] Rahkila, P. Grain - A Java data analysis system for

Total Data Readout. *Nucl. Instrum. Methods Phys. Res. Sect. A* **595**, 637-642 (2008).

[61] Heine, F. et al. Proton and alpha radioactivity of very neutron deficient Te, I, Xe and Cs isotopes, studied after electrostatic separation. *Z. Phys. A* **340**, 225-226 (1991).

[62] Krane, K. S. *Introductory Nuclear Physics* (Wiley, 1987).

[63] Schmidt, K. H. A new test for random events of an exponential distribution. *Eur. Phys. J. A* **8**, 141-145 (2000).

Acknowledgements

This work was supported by the Swedish Research Council under Grant No. 2019-04880, the United Kingdom Science and Technology Facilities Council (STFC) under Grants No.ST/P003885/1, No.ST/V001035/1, No.ST/P004598/1 and No.ST/V001027/1, the EU 7th Framework Programme, Integrating Activities Transnational Access, project No.262010 ENSAR, and the Academy of Finland under the Finnish Centre of Excellence Programme (Nuclear and Accelerator Based Physics Programme at JYFL). We thank the JYFL Accelerator laboratory staff for excellent operation of the K130 cyclotron and D. Delion, R. Liotta, N. Sandulescu, and C. Qi for fruitful discussions.

Author contributions

All authors have contributed to the publication by variously being involved in the design and the construction of detectors, in writing software, in operating the detectors and acquiring the raw data. W.Z was main responsible for calibrating the sub-systems, data reduction, and analysing the processed data. B.C. and W.Z. wrote the manuscript with input from all the authors.

Competing interests

The authors declare no competing interests.